SLAC-PUB-1782
SSRP-Report No. 76/06
July 1976
(A)

PARAMETERS IN THE HELICAL WIGGLER AND SYNCHROTRON RADIATION

Gilbert Chu[†]

Stanford Synchrotron Radiation Project[‡]
and
Stanford Linear Accelerator Center
Stanford University
Stanford, CA 94305

(Submitted to J. Appl. Phys.)

[†]Address after September 1, 1976: Harvard Medical School

[‡]Partially supported by National Science Foundation Grant No. DMR73-07692 and the Energy Research and Development Administration.

ABSTRACT

It has been suggested that helical wigglers be installed in electron storage rings to increase the brightness of the synchrotron radiation. The results of Kincaid[1] are used to show how the radiation is critically affected by the wiggler parameters: current, bore radius, and period. Comparison is made to transverse wigglers and ordinary bending magnets. It is shown that a helical wiggler at SPEAR could produce photons of 3 Å and perhaps 2 Å with a large improvement in brightness.

I. Introduction

Synchrotron radiation is produced from electron storage rings because the electrons are forced to travel in a curved trajectory by bending magnets. The intensity and collimation of synchrotron radiation at high energy rings such as SPEAR have permitted scientists to perform many experiments which are impossible with conventional sources of electromagnetic radiation.

There are a number of ways to increase the number of photons even further. Obvious methods include the increase of electron current in an existing storage ring or the construction of a new ring capable of higher energies (such as PEP) or the construction of a new ring at the same energy with a smaller bending radius. Considerable attention has also been focused on the possibility of installing magnetic field devices in existing rings. Such devices, known as "wigglers", would produce extra photons by subjecting the electrons to additional violent accelerations along a section of their trajectory in the ring. The wigglers are designed such that the electrons would suffer little or no net deflection from the unperturbed trajectory after exiting from the wiggler region.

Transverse wigglers apply strong magnetic fields in an alternating periodic arrangement along the electron trajectory. The synchrotron radiation is characteristic of a circular trajectory, and is not fundamentally different from the radiation from a storage ring, except that the energy and intensity of the photons may be increased by using powerful magnets and by including a large number of periodic wiggles.

Helical wigglers consist of a double helix of wires carrying currents in opposite directions. The resultant magnetic field is transverse to the axis of the helix and rotates around the axis with the period of the helix.

The electron trajectory is also a helix with the same period.

Illustrations of the electron trajectories in a transverse wiggler and in a helical wiggler are shown in Figs. 1(a) and 1(b), respectively.

The radiation from a helical trajectory has radically different spectral characteristics from the radiation from a circular trajectory, thus offering exciting possibilities for research.[1] Furthermore, there is reason to believe that helical wigglers may be installed in a storage ring without destroying the circulating electron beam.[2] In this paper we review the properties of the radiation from helical wigglers and discuss the practical aspects of designing them for installation at an electron storage ring. We illustrate how the synchrotron radiation is affected in dramatic ways by the parameters of the wiggler: the radius, period, and current of the helix.

We compare the synchrotron radiation spectra from helical wigglers, transverse wigglers and normal storage ring bending magnets. Finally, we estimate the effect of the angular divergence of the electron beam at SPEAR on the brightness of radiation from the helical wiggler.

II. Properties of the Radiation from a Helical Wiggler

The radiation from a moving charge has a calculable distribution. For a single electron moving through space, the energy radiated per unit solid angle per unit frequency interval is given by[3]

$$\frac{dI(\omega)}{d\Omega} = \frac{e^2\omega^2}{4\pi^2 c}\left|\int_{-\infty}^{\infty} \hat{n}\times(\hat{n}\times\vec{\beta})\, e^{i\omega(t-[\hat{n}\cdot\vec{r}(t)/c])}\, dt\right|^2$$

where $\vec{r}(t)$ and $c\vec{\beta}(t)$ are the position and velocity of the electron in some fixed coordinate system, and $\hat{n}$ is the unit vector from the origin of the coordinate system to the observer.

From this expression, Kincaid has computed the radiation from an electron traveling in a helical trajectory.[1] We shall summarize his results, following his notation.

For an electron traveling through a helical wiggler of period λ_o and producing a transverse magnetic field B on axis, with the assumptions that the electron energy is much larger than its mass

$$\gamma \equiv \frac{E_e}{m_e c^2} \gg 1$$

and that the number of periods in the wiggler is large

$$N \gg 1$$

Kincaid finds that the energy radiated per unit solid angle per unit frequency interval is[1]

$$\frac{dI(\omega)}{d\Omega} = \frac{e^2\, K^2\, \omega^2}{\pi^2 c\, \gamma^2\, \omega_o^2}\sum_{n=1}^{\infty}\left[J_n'^2(x) + \left(\frac{\gamma\theta}{K} - \frac{n}{x}\right)^2 J_n^2(x)\right]\times\frac{\sin^2 N\pi\left(\frac{\omega}{\omega_1} - n\right)}{\left(\frac{\omega}{\omega_1} - n\right)^2} \qquad (1)$$

where the angle θ is with respect to the axis of the helix,

$$x = \frac{K\theta}{\gamma} \frac{\omega}{\omega_o}$$

$$\omega_1 = \frac{\omega_o}{1 - \beta\sqrt{1 - \left(\frac{K}{\gamma}\right)^2}\cos\theta} \simeq \frac{2\gamma^2\omega_o}{1 + K^2 + \gamma^2\theta^2} \qquad (2)$$

and J_n and J_n' are the n^{th} order Bessel function and its derivative. Here

$$\omega_o = \frac{2\pi c}{\lambda_o}\beta\sqrt{1 - \left(\frac{K}{\gamma}\right)^2} \qquad \left(\beta^2 = 1 - \frac{1}{\gamma^2}\right)$$

is the circular frequency of the electron's helical orbit. The dimensionless magnetic field parameter K is defined by

$$K = \frac{e\lambda_o B}{2\pi m_e c^2} \qquad (3)$$

Note that the intensity of radiation depends on the <u>product</u> of the helical period λ_o and the magnetic field B. This is of critical importance in considering the design of the wiggler, as we shall see later.

At a given angle θ, the spectrum consists of a series of harmonics of the fundamental frequency ω_1. For $\theta = 0$, only the fundamental frequency contributes, and all the radiation occurs in a narrow peak at

$$\omega = \omega_1 \simeq \frac{2\gamma^2\omega_o}{1 + K^2} \qquad . \qquad (4)$$

The corresponding wavelength is

$$\lambda \simeq \frac{\lambda_o}{2\gamma^2}(1 + K^2) \tag{5}$$

The on axis intensity is easily computed from Eq. (1).

$$\left.\frac{dI(\omega)}{d\Omega}\right|_{\substack{\omega=\omega_1 \\ \theta=0}} = \frac{2N^2e^2\gamma^2K^2}{c(1+K^2)^2} \tag{6}$$

This expression is sharply peaked at $K = 1$, with the value

$$\left.\frac{dI(\omega)}{d\Omega}\right|_{\substack{\omega=\omega_1 \\ \theta=0 \\ K=1}} = \frac{N^2e^2\gamma^2}{2c} \tag{7}$$

The angular distribution of the radiated power may be computed by integrating Eq. (1) over all frequencies:

$$\int_o^\infty \frac{dI(\omega)}{d\Omega}\,d\omega = \frac{8Ne^2\omega_o\gamma^4}{c(1+K^2+\gamma^2\theta^2)^3} \sum_{n=1} n^2\left[J_n'^2(x_n) + \left(\frac{\gamma\theta}{K} - \frac{n}{x_n}\right)^2 J_n^2(x_n)\right] \tag{8}$$

where $x_n = \dfrac{2Kn\gamma\theta}{1 + K^2 + \gamma^2\theta^2}$.

This expression is valid in the limit of large N with $\theta \neq 0$. Kincaid has plotted the angular distribution of the radiated power from Eq. (8), and

his results are reproduced in Fig. 2.[1] For $K \geq 1$, the power maximum does not occur on axis but slightly off axis at an angle $\theta \simeq K/\gamma$. Although the power on axis decreases as K grows larger than unity, the power at $\theta \simeq K/\gamma$ increases dramatically. One may be tempted to consider using the radiation on the surface of the cone at $\theta \simeq K/\gamma$.

However, from Eq. (1), it is clear that higher harmonics contribute off-axis. The angular distribution of the radiation at the fundamental frequency $\omega = \omega_1$ is computed from Eq. (1),

$$\left.\frac{dI(\omega)}{d\Omega}\right|_{\omega=\omega_1} = \frac{4e^2\gamma^2K^2N^2}{c(1+K^2+\gamma^2\theta^2)^2}\left[J_1'^2(x) + \left(\frac{\gamma\theta}{K} - \frac{1}{x}\right)^2 J_1^2(x)\right] \qquad (9)$$

where $x = \dfrac{2K\gamma\theta}{1 + K^2 + \gamma^2\theta^2}$.

The angular distribution for the radiated power at the fundamental frequency is shown in Fig. 3 for different values of the magnetic field parameter K .

By comparing Figs. 2 and 3, we see that although the total power radiated may be greatest at $\theta \simeq K/\gamma$ (for $K \gtrsim 1$) , the power radiated at the fundamental frequency is always greatest on axis. The radiation off axis contains the higher frequency harmonics and at $\theta \simeq K/\gamma$, radiated frequencies are spread over a broad range.

III. Considerations for the Design of a Helical Wiggler

Because of the strong dependence of the intensity of radiation on the parameter K in Eq. (6), there are strong restrictions on the practical design of a helical wiggler. For an ideal wiggler wound as a double helix of wires carrying current in opposite directions, the transverse field on axis is,[4]

$$B = \frac{8\pi I}{10\lambda_o}\left[\frac{2\pi a}{\lambda_o} K_o\left(\frac{2\pi a}{\lambda_o}\right) + K_1\left(\frac{2\pi a}{\lambda_o}\right)\right] \tag{10}$$

The wiggler dimensions are determined by the radius of the helix a, and its wavelength λ_o, both measured in centimeters. The current I is in amps and B is in Gauss. The functions K_o and K_1 are modified Bessel functions.

The radiation depends not on the magnetic field B alone, but on the magnetic field parameter K. Combining Eqs. (3) and (10),

$$\begin{aligned} K &= \left(\frac{2e}{5m_e c^2}\right) I \left[\xi K_o(\xi) + K_1(\xi)\right] \\ &= 1.87\, I \left[\xi K_o(\xi) + K_1(\xi)\right] \end{aligned} \tag{11}$$

where I is expressed in amps, and where K depends only on the ratio of bore radius and wavelength of the helix, the dimensionless helix parameter,

$$\xi = \frac{2\pi a}{\lambda_o} \tag{12}$$

Again, I is measured in amps. The modified Bessel functions K_o and K_1 both fall sharply as ξ increases. In fact for small ξ ,

$$K_o(\xi) \simeq -\ln \xi$$

$$K_1(\xi) \simeq \frac{1}{4\xi}$$

and for large ξ both K_o and K_1 fall faster than exponents.[5]

The wiggler must be designed so that the parameter $K = 1$, by Eq. (6). In the practical installation of a wiggler in a storage ring, there is a lower limit on the bore radius a . (At SPEAR the limits are 5 cm in the 3 meter straight sections and about 1.5 cm in the 2 meter interaction regions.) Thus, if a given wavelength λ_o for the helix is desired, the wiggler current I must be adjusted accordingly. However, there is a very strong lower limit to λ_o because of the strong dependence of the modified Bessel functions on the helix parameter ξ . In particular, as ξ increases (for decreasing λ_o), I increases faster than exp (ξ) . The limits of superconducting technology are quickly reached.

A series of curves showing the radiation intensity as a function of the helix parameter ξ for different values of the current is shown in Fig. 4. Once the wiggler has been built and the helix dimensions are fixed, a very narrow range of currents will provide optimal intensities. Conversely, the practical upper limit on currents achievable with present day technology sets a stringent upper limit on the helix parameter ξ . A graph of the optimal

current as a function of the helix parameter ξ is shown in Fig. 5. We have roughly indicated the technological threshold.[6]

The parameters of the wiggler are the wiggler current I, the helix wavelength λ_o, and the bore radius a. Once they have been adjusted such that the magnetic field parameter $K = 1$ in Eq. (11), the brightness will be maximized at a fixed value depending only on the number of periods N and the beam energy E_e. As an example, Fig. 5 indicates that the brightness from a one million amp wiggler will be identical to the brightness from a ten amp wiggler, as long as the parameter K is fixed at unity. In fact, by Eq. (1), the radiation spectra from the two wigglers will be identical.

Once the wavelength λ_o of the wiggler is determined, and the current is adjusted to optimize performance, the wavelength of the emitted radiation may be computed from Eq. (5),

$$\lambda = \lambda_o/\gamma^2 \tag{13}$$

The shortest wavelength of the X-rays is fixed by the highest energy for the electrons in the storage ring.

For $K = 1$ and for a given bore radius a, the helix wavelength λ_o is determined by the current in the wiggler in Eqs. (11) and (12).

$$\lambda_o = 2\pi a/\xi_{K=1}(I)$$

The helix wavelength as a function of wiggler current is plotted in Fig. 6 for different values of the bore radius. The wavelength of the produced radiation corresponding to electron beam energy $E_e = 4$ GeV is shown on the left hand axis.

The nature of the curves permits some dramatic conclusions. For example, if the bore radius $a = 3$ cm, photons of wavelength 2 Å may be produced only by using a superconducting wiggler carrying a large current of 300,000 amps. On the other hand, photons of 4 Å are produced using a conventional current of only 200 amps!

IV. Comparison of Spectra

The synchrotron radiation spectrum from a helical wiggler may be compared to the spectra from a storage ring and from a transverse wiggler. Here, we shall compute the photon flux from the helical wiggler on axis ($\theta = 0$) and compare it to the fluxes from the storage ring and transverse wiggler in the plane of the electron trajectory. Other comparisons are given in Kincaid's paper.[1]

For a normal bending magnet, the brightness function is[3]

$$\left.\frac{dI(\omega)}{d\Omega}\right|_{\theta=0} = \frac{3e^2}{4\pi^2 c}\gamma^2 r^2 K_{2/3}^2(r/2) \qquad (14)$$

where $r = \omega/\omega_c$ and

$$\omega_c = \frac{3c}{2}\gamma^3/\rho \quad . \qquad (15)$$

The cyclotron radius ρ of the electron beam is,

$$\rho = \frac{m_e c^2}{e} \frac{\gamma\beta}{B} \quad .$$

The spectrum from a storage ring of fixed radius $\rho = 12.7$ m (e.g. SPEAR) is shown in Fig. 7 for various electron beam energies.

In a transverse wiggler, the magnetic field B may be adjusted in such a way that the function $r^2 K^2_{2/3}(r/2)$ remains fixed at its maximum value. Of course, as the photon energy increases, there will be a point at which the magnetic field will reach its maximum value, and then the spectrum will fall off with a shape characteristic of a normal bending magnet. The spectrum from a transverse wiggler with 6 poles (3 periods) and with a maximum magnetic field of 50 kG is also shown in Fig. 7 for various beam energies.

The brightness from a helical wiggler with 100 turns and a total length of 2 meters is also shown. Of course, at a given beam energy, only a single photon energy is radiated at $\theta = 0$. At any fixed beam energy, there is a potential improvement in brightness of almost 10^5 over the storage ring and of 10^4 over the transverse wiggler.

Notice that if photon energy is of prime importance, the helical wiggler suffers in comparison to the conventional devices as the electron beam energy increases. For a bending magnet or transverse wiggler, the critical photon energy increases with the third power of the beam energy, by Eq. (15).

On the other hand, for a helical wiggler, the photon energy only increases with the square of the beam energy, by Eq. (4).

V. Brightness Attenuation from Beam Divergences

The angular divergence of the electron beam can seriously affect the performance of the helical wiggler. If the beam divergence is described by a Gaussian,

$$P(\theta) = \frac{1}{2\pi\sigma^2} e^{-\frac{1}{2}(\theta/\sigma)^2}$$

then Kincaid[1] finds the brightness of the fundamental frequency at $\theta = 0$ is reduced by the factor $2N\gamma^2\sigma^2$.

At SPEAR, the beam divergence depends strongly on position around the ring. The beam divergences $\sigma_{x'}$ and $\sigma_{y'}$ in the horizontal and vertical directions at a beam energy of 3 GeV are given in Table I. The numbers are expressed in milliradians, and it is assumed that the beam energy is 3 GeV . The normal configuration corresponds to the normal operation of SPEAR in which electrons but not positrons are stored in the ring. The high brightness configuration corresponds to operation in which the production of synchrotron light is optimized. The values of $\sigma_{x'}$ and $\sigma_{y'}$ in the normal configuration are actual beam parameters at SPEAR; the values in the high brightness configuration are estimates based on a feasibility study.

In the transverse wiggler and fixed radius bending magnet the brightness attenuation due to beam divergence is $\gamma\sigma_{y'}$. Using the values in

Table I, we see that $\gamma\sigma_{y'} \lesssim 1$ at SPEAR. Therefore there is little attenuation in the transverse wiggler or bending magnet.

In the helical wiggler, Blewett and Chasman[2] find that for zero initial beam divergence, the helical wiggler introduces oscillations which correspond to a beam divergence roughly equal to the pitch angle in the beam orbit,

$$\theta_{pitch} \simeq K/\gamma \quad .$$

If an axial field is introduced, the oscillations can be made to disappear.

Thus we assume that the introduction of the helical wiggler into the beam will not change the existing beam divergences, and we calculate the corresponding reduction in brightness on axis. The angular distribution is the product of two Gaussians,

$$P(x', y') \sim e^{-\frac{1}{2}(x'/\sigma_{x'})^2} e^{-\frac{1}{2}(y'/\sigma_{y'})^2} \tag{16}$$

Transformation to polar coordinates gives,

$$P(\theta,\varphi) \sim \exp\left[-\frac{\theta^2}{2}\left(\cos^2\varphi/\sigma_{x'}^2 + \sin^2\varphi/\sigma_{y'}^2\right)\right]$$

$$x' \simeq \theta\cos\varphi \quad , \qquad y' \simeq \theta\sin\varphi$$

Integration over azimuthal angle gives,

$$P(\theta) = \int_0^{2\pi} d\varphi\, P(\theta,\varphi) \sim 2e^{-\frac{1}{2}\theta^2/\sigma_{x'}^2} \int_0^2 dt\, \frac{e^{-(s\theta^2)t}}{\sqrt{t(2-t)}}$$

where
$$s = \frac{1}{4}\left(\frac{1}{\sigma_{y'}^2} - \frac{1}{\sigma_{x'}^2}\right) > 0 \qquad (17)$$

and we have made the change of variables,

$$t = 2\sin^2\varphi \quad .$$

The definite integral is known[8] to have the value $\pi e^{-s\theta^2} I_o(s\theta^2)$, and we finally obtain,

$$P(\theta) \sim 2\pi\, e^{-r\theta^2} I_o(s\theta^2) \qquad (18)$$

where
$$r = \frac{1}{4}\left(\frac{1}{\sigma_{y'}^2} + \frac{1}{\sigma_{x'}^2}\right) \qquad (19)$$

and I_o is the modified Bessel function, which increases monotonically somewhat slower than an exponential as its argument increases. We estimate the effective beam divergence by defining σ_{eff} by the relation

$$e^{-r\sigma_{eff}^2} I_o\left(s\sigma_{eff}^2\right) = \frac{1}{2} \quad . \qquad (20)$$

The results are shown in Table I. Since $\sigma_{y'} \ll \sigma_{x'}$, we expect to find σ_{eff} to be slightly larger than $\sigma_{y'}$ and much smaller than $\sigma_{x'}$.

If the helical wiggler is built with 100 periods, the corresponding reductions in brightness at 3 GeV are shown in Table I. The differences are quite large and strongly suggest the use of the helical wiggler in the straight section under the high brightness configuration. Unfortunately, the allowable bore radius in the straight section is more than three times larger than in the interaction region. Perhaps the best solution would be the use of focusing inserts in the interaction region to achieve a smaller angular divergence in the beam.

In the interaction region, the attenuation is a factor of 364 in the normal configuration. A practical helical wiggler in this region would have a bore radius of about 3 cm ,[6] a period of about 2 cm , and a total length of 2 m . By consulting Fig. 7, we see that the helical wiggler would offer a factor of 150 gain in brightness at SPEAR while producing 3 Å radiation.

In the straight section, the attenuation can become negligible in the high brightness configuration. A practical wiggler would have a bore radius of about 6 cm ,[6] a period of 3 cm , and a total length of 3 m . The wiggler could increase the brightness by a factor of 55,000, while producing 5 Å radiation.

VI. Conclusion

We conclude by emphasizing that the special properties of the helical wiggler demand careful attention to its design for installation in a storage

ring. The most important curves in this paper are displayed on log-log axes, and oftentimes small gains in performance may be achieved only by huge increases in technology. However, we have found that wavelengths of 3 Å and perhaps 2 Å may be produced from a helical wiggler at SPEAR with large increases in brightness over the unmodified storage ring.

The installation of a helical wiggler at a higher energy machine could result in the production of synchrotron radiation with much shorter wavelengths. At PEP[9], the maximum beam energy will be 4 times larger than at SPEAR and the corresponding photon wavelengths could be 16 times shorter.

Of course, further study is required on the practical aspects of actually installing such a device in a storage ring. Guarding against beam instabilities, minimizing the beam divergence, and many other items are all important engineering problems that must be addressed and solved.

The author gratefully acknowledges stimulating conversations with Herman Winick who suggested studying the possibility of installing a helical wiggler at SPEAR, with Steven St. Lorant who was enthusiastic about building one, and with Philip Morton about machine physics at SPEAR. The work in this paper was partially supported by National Science Foundation Grant No. DMR73-07692, in cooperation with the Stanford Linear Accelerator and the U. S. Energy Research and Development Administration. The author also thanks S. D. Drell and the Theoretical Physics Group at SLAC for the warm atmosphere in which much of the work here was done.

TABLE I

Beam Divergences and Brightness Attenuation

(E_e = 3 GeV , N = 100)

	$\sigma_{x'}$ (mrad)	$\sigma_{y'}$ (mrad)	σ_{eff} (mrad)	Attenuation Factor
Normal Configuration				
Interaction Point	.65	.19	.23	364
3 m Straight Section	.18	.044	.055	21
High Brightness Configuration				
Interaction Point	.35	.065	.084	49
3 m Straight Section	.080	.010	.013	1.2

APPENDIX

Units for Radiation Intensity

In Jackson's notation,[3] the expression $dI(\omega)/d\Omega$ represents the energy radiated per unit solid angle per unit frequency interval per electron. To convert to units which are of interest in calculating synchrotron radiation spectra we write:

$$\frac{\text{Number of photons}}{\text{sec} \times 1\% \text{ bandwidth} \times \text{ma of electron current} \times (\text{mrad})^2}$$

$$= \frac{dI(\omega)}{d\Omega} \left(\frac{\text{energy}}{\text{radian}^2 \times \text{frequency interval} \times \text{electron}} \right)$$

$$\times \; 10^{-6} \left(\frac{\text{radian}^2}{\text{mrad}^2} \right) \times \frac{1}{\hbar\omega} \left(\frac{1}{\text{energy/photon}} \right)$$

$$\times \; 10^{-2}\omega \left(\frac{1}{1\% \text{ bandwidth/frequency interval}} \right)$$

$$\times \frac{I}{e} \left(\frac{\text{electrons}}{\text{sec}} \right) \times \frac{1}{10^3 I} \left(\frac{1}{(\text{ma/amp}) \times \text{amps}} \right)$$

$$= \left[\frac{dI(\omega)}{d\Omega} \frac{1}{e^2/c} \right] \times \frac{e^2}{\hbar c} \times \frac{1}{e} \times 10^{-11}$$

$$= \left[\frac{dI(\omega)}{d\Omega} \frac{1}{e^2/c} \right] \times \frac{1}{137} \times \frac{1}{1.6 \times 10^{-19}} \times 10^{-11}$$

$$= \left[\frac{dI(\omega)}{d\Omega} \frac{1}{e^2/c} \right] \times 4.56 \times 10^5$$

Thus, when converting from (energy/solid angle/frequency interval/electron) to the more practical units of (photons/sec/1% bandwidth/ma/mrad^2) simply replace the constant e^2/c by the number 4.56×10^5 in the expression for $dI(\omega)/d\Omega$.

REFERENCES

1. B. Kincaid, Bell Laboratories preprint (1976) submitted to J. Appl. Phys.
2. J. P. Blewett and R. Chasman, Brookhaven National Laboratory preprint (1976), submitted to J. Appl. Phys.
3. J. D. Jackson, Classical Electrodynamics, p. 480, John Wiley and Sons (1965).
4. W. R. Smythe, Static and Dynamic Electricity, p. 277, McGraw Hill (1950).
5. M. Abramowitz and I. Stegun, Handbook of Mathematical Functions, U. S. Government Printing Office (1964).
6. S. St. Lorant, private communication.
7. H. Winick, private communication.
8. I. S. Gradshteyn and I. M. Ryzhik, Table of Integrals, Series and Products, p. 315, line 3.364, Academic Press (1965).
9. PEP is the Lawrence Berkeley Laboratory/Stanford Linear Accelerator Center 18 GeV colliding beam storage ring, now under construction. The aperture requirements for the electron beam at PEP will be similar to those at SPEAR.

FIGURE CAPTIONS

Figure 1 -- Trajectories from (a) a transverse wiggler and (b) a helical wiggler.

Figure 2 -- Angular distribution of the radiated power (from Ref. 1).

Figure 3 -- Angular distribution of the radiation at the fundamental frequency $(\omega = \omega_1)$.

Figure 4 -- Intensity of the radiation on axis $(\theta = 0)$ vs the helix parameter ξ for different values of the wiggler current.

Figure 5 -- Optical wiggler current vs helix parameter.

Figure 6 -- Helix wavelength and photon wavelength vs wiggler current for different values of the bore radius.

Figure 7 -- Comparison of the idealized spectral distributions for the helical wiggler, transverse wiggler and fixed radius bending magnet (SPEAR).

(a)

(b)

Fig. 1

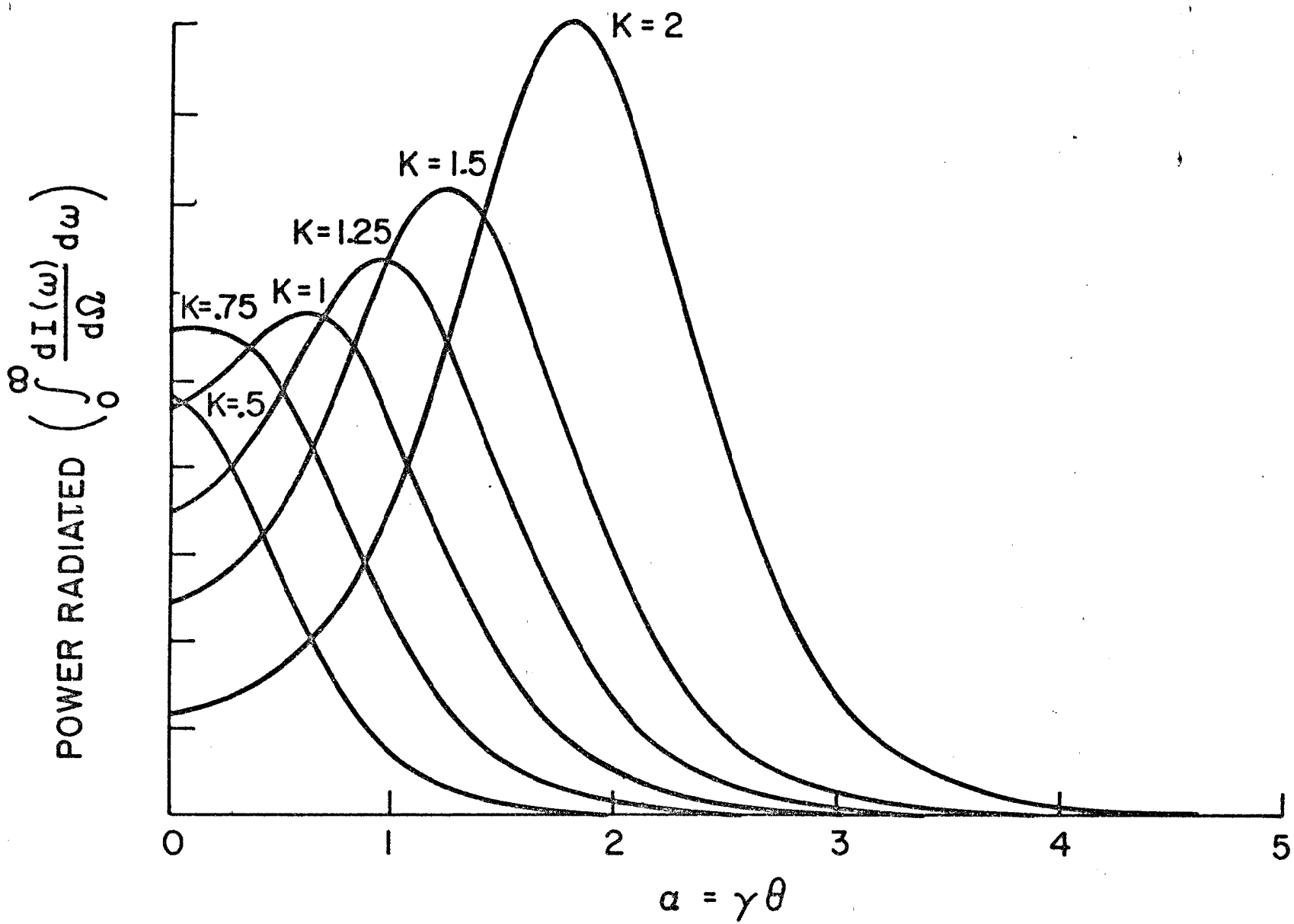
K = 2
K = 1.5
K=1.25
K=1
K=.75
K=.5
POWER RADIATED $\left(\int_0^\infty \frac{dI(\omega)}{d\Omega} d\omega\right)$
0
1
2
3
4
5
$a = \gamma\theta$

Fig. 2

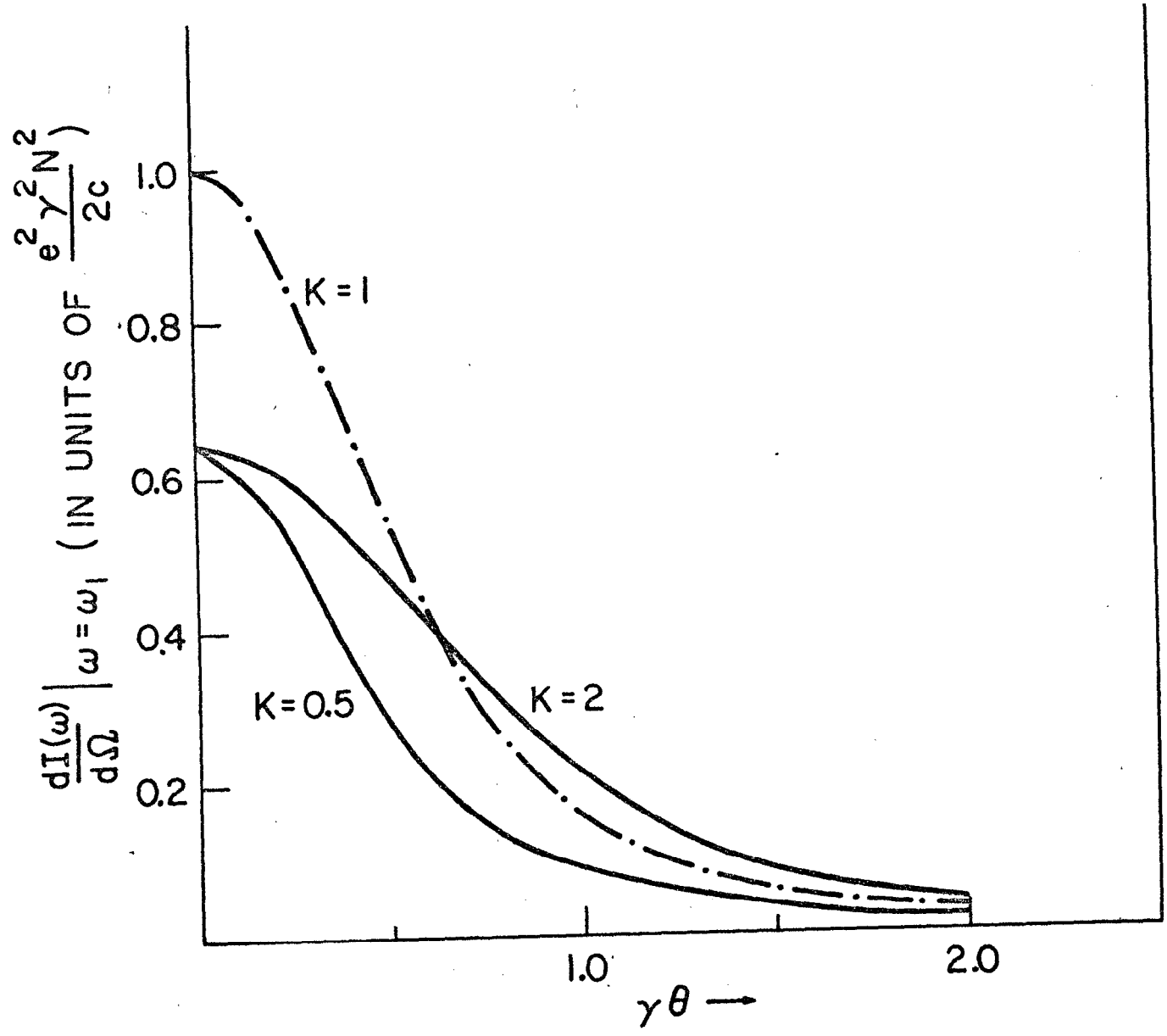
$\frac{dI(\omega)}{d\Omega}\Big|_{\omega=\omega_1}$ (IN UNITS OF $\frac{e^2\gamma^2N^2}{2c}$)
1.0
0.8
0.6
0.4
0.2
K = 1
K = 2
K = 0.5
1.0
2.0
$\gamma\theta$ →

Fig. 3

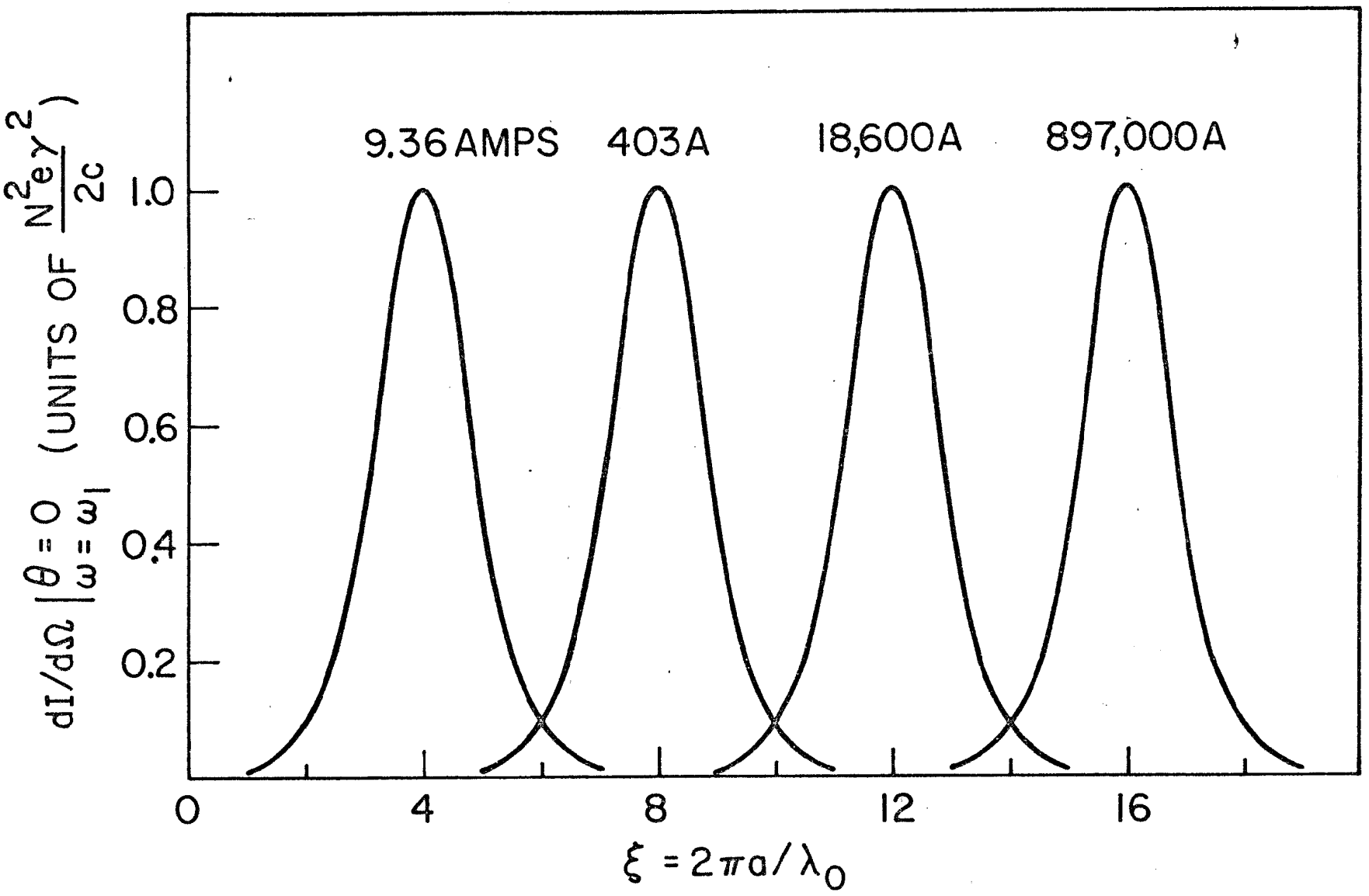
9.36 AMPS
403A
18,600A
897,000A
dI/dΩ |θ=0 ω=ω1 (UNITS OF N²eγ²/2c)
1.0
0.8
0.6
0.4
0.2
0
4
8
12
16
ξ = 2πa/λ0

Fig. 4

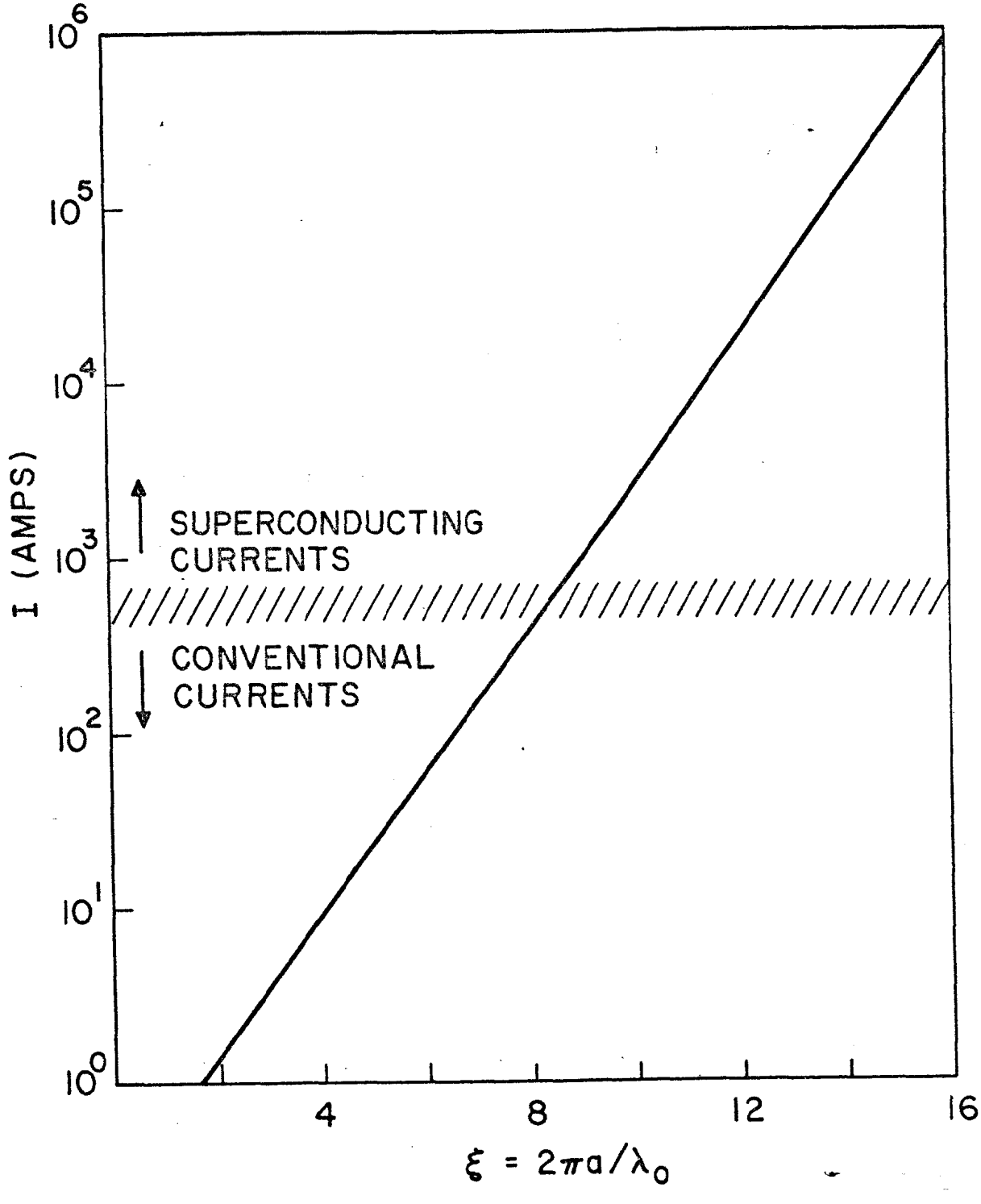
10^6
10^5
10^4
10^3
10^2
10^1
10^0
I (AMPS)
SUPERCONDUCTING CURRENTS
CONVENTIONAL CURRENTS
4
8
12
16
$\xi = 2\pi a/\lambda_0$

Fig. 5

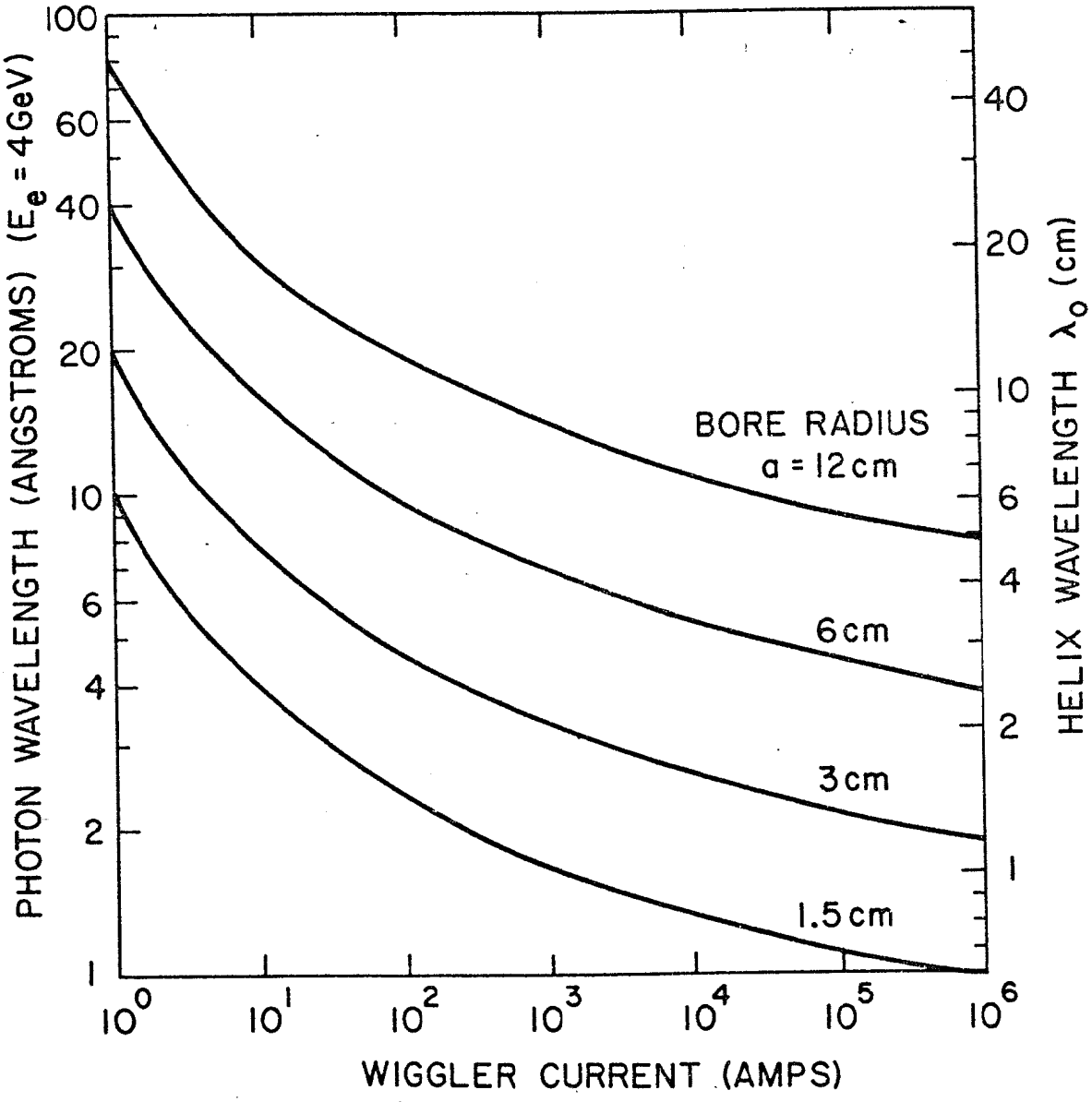
PHOTON WAVELENGTH (ANGSTROMS) (E_e = 4GeV)
HELIX WAVELENGTH λ_o (cm)
WIGGLER CURRENT (AMPS)
BORE RADIUS
a = 12cm
6cm
3cm
1.5cm
100
60
40
20
10
6
4
2
1
40
20
10
6
4
2
1
10^0
10^1
10^2
10^3
10^4
10^5
10^6

Fig. 6

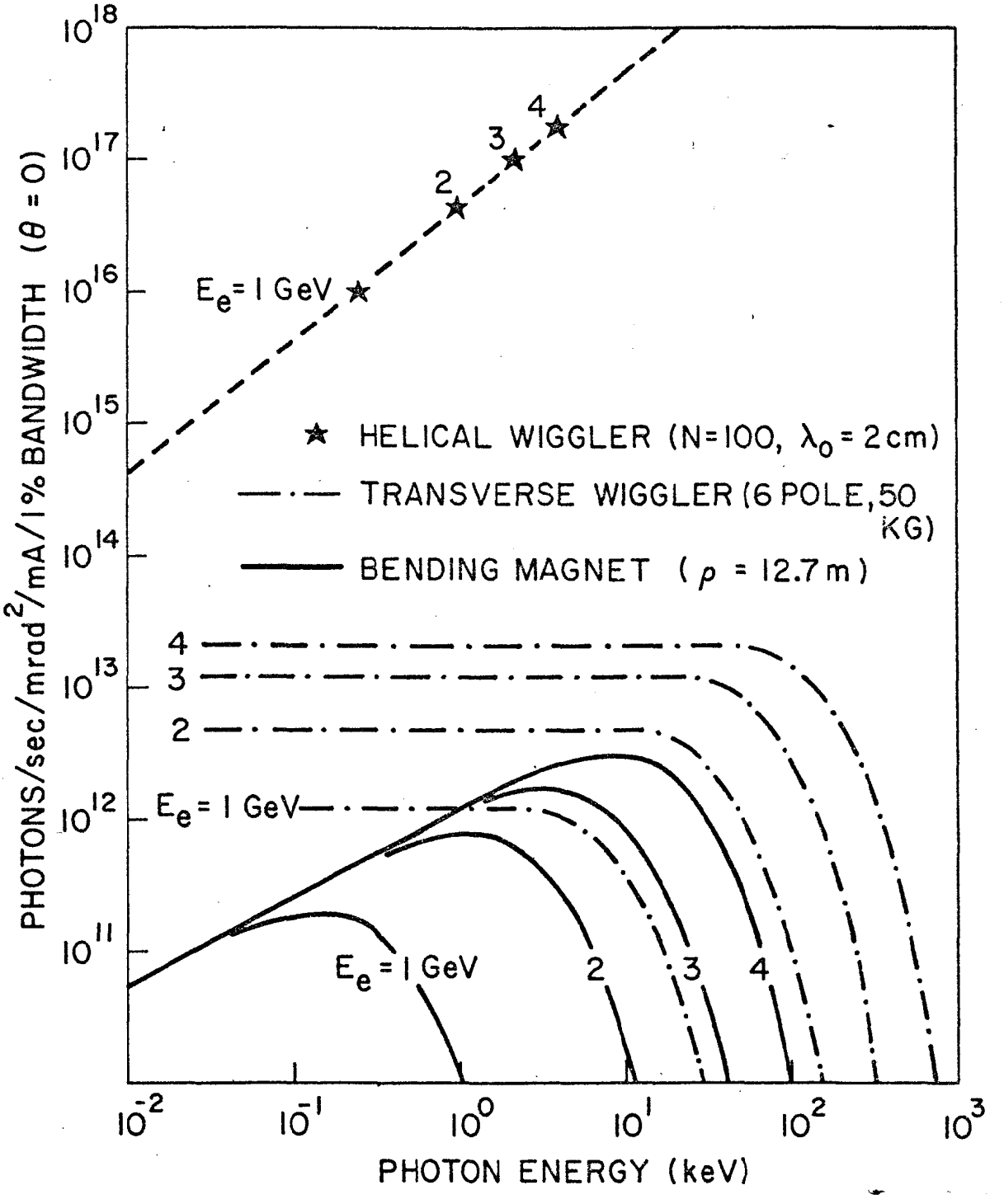
PHOTONS/sec/mrad²/mA/1% BANDWIDTH (θ = 0)
PHOTON ENERGY (keV)
HELICAL WIGGLER (N=100, λ0 = 2cm)
TRANSVERSE WIGGLER (6 POLE, 50 KG)
BENDING MAGNET (ρ = 12.7m)
Ee = 1 GeV
2
3
4

Fig. 7